Geochimica et Cosmochimica Acta, Vol. 69, No. 19, pp. 4719–4732, 2005

0016-7037/05 $30.00 + .00

doi:10.1016/j.gca.2005.06.014

Trace element compositions of submicroscopic inclusions in coated diamond: A tool for understanding diamond petrogenesis

Emma Tomlinson,[1,*] Isabel De Schrijver,[2] Katrien De Corte,[3] Adrian P. Jones,[1] Luc Moens,[2] and Frank Vanhaecke[2]

[1]Department of Earth Sciences, University College London, Gower Street, London WC1E 6BT, United Kingdom
[2]Department of Analytical Chemistry, Ghent University, Proeftuinstraat 86, B-9000 Ghent, Belgium
[3]Raad voor Diamant (HRD), Gem Defence Initiative Department (GDI), Plaslaar 50, B-2500 Lier, Belgium

(*Received October* 19, 2004; *accepted in revised form June* 20, 2005)

Abstract—Trace element compositions of submicroscopic inclusions in both the core and the coat of five coated diamonds from the Democratic Republic of Congo (DRC, formerly Zaire) have been analyzed by Laser Ablation Inductively Coupled Mass Plasma Spectrometry (LA-ICP-MS). Both the diamond core and coat inclusions show a general 2–4-fold enrichment in incompatible elements relative to major elements. This level of enrichment is unlikely to be explained by the entrapment of silicate mantle minerals (olivine, garnet, clinopyroxene, phlogopite) alone and thus submicroscopic fluid or glass inclusions are inferred in both the diamond coat and in the gem quality diamond core. The diamond core fluids have elevated High Field Strength Element (Ti, Ta, Zr, Nb) concentrations and are enriched in U relative to inclusions in the diamond coats and relative to chondrite. The core fluids are also moderately enriched in LILE (Ba, Sr, K). Therefore, we suggest that the diamond cores contain inclusions of silicate melt. However, the Ni content and Ni/Fe ratio of the trapped fluid are very high for a silicate melt in equilibrium with mantle minerals; high Ni and Co concentrations in the diamond cores are attributed to the presence of a sulfide phase coexisting with silicate melt in the diamond core inclusions. Inclusions in the diamond coat are enriched in LILE (U, Ba, Sr, K) and La over the diamond core fluids and to chondrite. The coats have incompatible element ratios similar to natural carbonatite (coat fluid: Na/Ba ≈0.66, La/Ta≈130). The coat fluid is also moderately enriched in HFSE (Ta, Nb, Zr) when normalized to chondritic Al. LILE and La enrichment is related to the presence of a carbonatitic fluid in the diamond coat inclusions, which is mixed with a HFSE-rich hydrous silicate fluid similar to that in the core. The composition of the coat fluid is consistent with a genetic link to group 1 kimberlite. *Copyright © 2005 Elsevier Ltd*

1. INTRODUCTION

Fluids and melts play an important role in many mantle processes. They are responsible for the transport of volatiles between mantle reservoirs; this strongly influences the trace element and isotopic signatures of those reservoirs and also causes metasomatism. Fluids control the stability fields and solidus temperatures of major minerals and stabilize carbonate and hydrous minerals. In addition, C-O-H fluids are an important carbon source and may be a catalyst for diamond growth. Therefore, direct samples of mantle volatiles are valuable sources of information about conditions during diamond growth. Diamond is mechanically strong and has a low reactivity in silicate environments, so that mantle fluids trapped as inclusions are preserved unaltered during subsequent metasomatic events and kimberlite eruption.

Coated diamonds comprise a non-fibrous octahedral core and an overgrowth of inclusion-rich fibrous diamond. Carbon isotope compositions in the diamond lattice provide a record of the carbon source for diamond growth. $\delta^{13}C$ values for non-fibrous diamonds, such as the diamond cores, span a wide range (−4 to −23‰), while fibrous diamond compositions, such as the coat, are restricted; −5 to −8‰, (Boyd et al., 1992; Snyder et al., 1995; Cartigny et al., 2001; Deines et al., 2001). Substitutional nitrogen in the diamond cores is often highly aggregated, suggesting long mantle residence times, while the fibrous coat has poorly-aggregated nitrogen pairs, suggesting that the diamond coats are significantly younger than their cores (Boyd et al., 1987). Inclusions in fibrous diamonds may retain a residual internal pressure of 1.4 to 2.0 GPa, corresponding to a formation pressure of 4–7 GPa (calculated at 1000–1300°C; Navon, 1991). This is comparable to the conditions of non-fibrous diamond growth at 900–1300°C and 4–6 GPa (Meyer, 1987; Harris, 1992), derived from geothermobarometry of silicate inclusions. Therefore, these fibrous diamonds must grow at depth under similar conditions to the growth of the diamond core, rather than during kimberlite ascent. However, the similarity between the Sr isotope compositions of fibrous diamonds from Mbuji Mayi (DRC) and of their host kimberlite suggests a genetic link between kimberlite petrogenesis and the fibrous diamond growth fluid (Akagi and Masuda, 1988).

Non-fibrous diamonds contain silicate, oxide and sulfide inclusions that originate from two main compositional mantle suites: peridotite and eclogite. An intermediate websteritic suite is also recognized. Fibrous diamonds contain quartz, apatite, carbonates, biotite and H_2O (Lang and Walmsley, 1983; Navon et al., 1988; Guthrie et al., 1991; Walmsley and Lang, 1992a,b). Combined Electron Microprobe Analysis (EMPA) and infrared spectroscopy of inclusions in fibrous diamonds has identified three end-member fluid compositions: 1) a carbonatite-like fluid enriched in Ca, P and CO_2, 2) a silicate fluid rich in Si, Al, K and H_2O (Navon et al., 1988; Schrauder and Navon, 1994), and 3) a KCl-H_2O "brine" (Izraeli et al., 2001, 2004). There is

* Author to whom correspondence should be addressed (emma.tomlinson@ucl.ac.uk).

Table 1. Summary of bulk physical and spectral characteristics of the diamond core and coat regions.[a]

Sample	ct.	core %N as IaB	core N (ppm)	Color	N (ppm)	H_2O (ppm)	Coat CO_2 (ppm)	CO_2#	Minerals present
CTPb8	0.223	23	1480	Gray-white	1365	108	22	17	carb.
CTPs2	0.059	65	890	Milky while	1137	126	40	33	carb. apatite
CTPs13	0.071	27	4	Yellow	<20	48	5	10	quartz, carb.
CTPs14	0.017	—	—	Dark green	1753	401	172	32	carb. quartz, apatite
CDR3	0.061	—	—	Gray-green	1370	182	—	—	quartz

[a] Sample weight in carats (1 ct = 0.2 g), nitrogen, H_2O, and CO_2 concentrations in ppm; $CO_2\# = CO_2/(CO_2 + H_2O)$; % N as IaB is the percentage of nitrogen present in B defects.

a continuum of compositions between the carbonate and silicate end-members (Navon et al., 1988; Schrauder and Navon, 1994) and also between carbonatite and brine (Klein-BenDavid et al., 2004).

The trace element compositions of octahedral diamonds (Fesq et al., 1975; Bibby, 1982; Damarupurshad et al., 1997) and fibrous diamonds (Akagi and Masuda, 1988; Schrauder et al., 1996; Damarupurshad et al., 1997) have previously been analyzed by instrumental neutron activation analysis (INAA). Wang et al. (2003) used LA-ICP-MS to analyze the trace element composition of inclusions in a single fibrous diamond coat. Here we report trace element data obtained by LA-ICP-MS from across both the core and coat of five coated diamonds. The aim of this study is to identify the source of impurities in the fibrous coat and the non-fibrous core, and to compare the compositions of submicroscopic inclusions in these regions. We will also address the question of whether there is a genetic relationship between the coat fluid and kimberlite magma.

2. SAMPLES AND ANALYTICAL METHODS

2.1. Samples

The sample group comprises five coated diamonds from the Democratic Republic of Congo (DRC), probably from the Mbuji Mayi kimberlite. The diamond cores are 2 to 4 mm in diameter and record numerous growth events, distinguished by truncated zoning in cathodoluminescense due to resorption and subsequent overgrowth. The diamond coats are several mm thick and are composed of a single growth zone indicating growth during one event. The samples were prepared by laser cutting and polished on both sides to form plates. Samples were cleaned in concentrated H_2SO_4 and rinsed with Milli-Q water prior to analysis. The sample characteristics are summarized in Table 1.

2.2. Analytical Method

2.2.1. LA-ICP-MS

Trace element compositions were analyzed by Laser Ablation Inductively Coupled Plasma Mass Spectrometry (LA-ICP-MS) at Ghent University, Belgium. The instrument used was a Perkin-Elmer SCIEX Elan 6100 quadropole based ICP-MS, equipped with a Lambda Physik COMPex 100 excimer laser and a GeoLas illumination system. The excimer laser operates at a wavelength of 193 nm and uses a gas mixture of Ar with 5% F_2 and small amounts of Ne. The following isotopes were analyzed in the coated diamonds: ^{23}Na, ^{27}Al, ^{39}K, ^{45}Sc, ^{47}Ti, ^{55}Mn, ^{57}Fe, ^{58}Ni, ^{59}Co, ^{69}Ga, ^{88}Sr, ^{90}Zr, ^{93}Nb, ^{138}Ba, ^{139}La, ^{181}Ta and ^{238}U. Masses 57 and 58 are subject to interference from Ar-O molecular species (e.g., $ArO(H)^+$) in the carrier gas, we have corrected for the effect of this contribution by subtracting the gas blank, which was measured for 30 s prior to each ablation.

In view of the low trace element concentrations in diamond, the maximum spot size (120 μm), the maximum frequency (20 Hz) and the maximum attainable energy (200 mJ) were used. The ablation time was 30 s (600 shots) at each point; the stability of the ^{13}C signal in Figure 1 (RSD $\approx$ 10 %) shows that it is possible to achieve controlled ablation of the sample over a period of 30 s. Surface contamination was avoided by cleaning the sample surface with 10 laser pulses before counting. Ablation generated sharp craters 45–50 μm in depth. The 120 μm diameter sample spot encompassed a multitude of micro-inclusions, therefore this is a bulk analytical technique. Traverses were taken across each specimen, with at least 4 sample positions in each coat and core. An example of a time-resolved plot of the raw data is shown in Figure 1. Data collected from ablation pits straddling fractures or the core-coat boundaries were discarded. The median composition in each sample region (core or coat) was taken as the representative value for that region; the median was used in preference to the mean in order to minimize the possible influence of outliers (e.g., due to silicate inclusions).

In calculating trace element concentrations, we have assumed that all impurities are located in micro-inclusions and not in the diamond lattice (e.g., Fesq et al., 1975; Bibby, 1982; Damarupurshad et al., 1997). LA-ICP-MS intensities were calibrated to element concentrations (in ppm) using NIST Standard Reference Material (SRM) 612 and the G-PROBE1 glass, a silicate glass designed as an international proficiency test for microprobe laboratories (Potts et al., 2002). In the absence of an internal standard, trace element concentrations have been calibrated to an assumed Al concentration of 8600 ppm, this is the Al concentration of carbonaceous (CI) chondrites (McDonough and Sun, 1995). This method does not give the absolute impurity concentration of the diamond because no carbon-based standard was used; conclusions are drawn from element ratios or concentrations relative to chondritic Al. The use of this arbitrary Al concentration gives a semi-quantitative estimate of composition of inclusions in the dia-

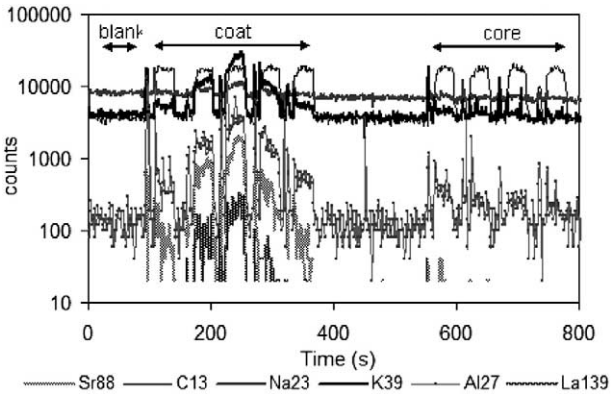

Fig. 1. Time-resolved data plot of sample CTPs2 (traverse a) showing selected elements (^{13}C, ^{23}Na, ^{27}Al, ^{39}K, ^{88}Sr, ^{139}La). Each point is ablated for 30 s. Each point is preceded by sharp peak due to preablation cleaning of sample spot.

Table 2. Median (shaded) trace element composition of diamond core fluids and compositions of fluid at individual LA-ICP-MS sample spots (unshaded).[a]

Sample	Na	K	Sc	Ti	Mn	Fe	Co	Ni	Ga	Sr	Zr	Nb	8a	La	Ta	U
error (3σ)	1365	197	88	100	29	349	6.6	102	1.3	5.2	4	2.6	4.1	1.0	2	3
CTPb8	21245	11545	3837	5215	n/d	6708	102	2068	84	385	90	43	276	62	n/d	n/d
8a	n/d	16197	3325	3103	n/a	n/d	n/d	n/d	69	1016	n/a	n/d	2840	143	n/a	n/a
9a	n/d	9959	4305	n/d	n/a	13567	147	3439	99	424	n/a	n/d	1765	55	n/a	n/a
10a	7090	13131	3369	4093	n/a	6708	76	1169	126	385	n/a	56	312	62	n/a	n/a
11a	35400	1305	5216	6337	n/a	3461	61	1129	55	83	n/a	43	241	43	n/a	n/a
1d	n/d	n/d	n/d	n/d	n/d	5402	n/d	n/d	n/d	n/d	90	n/d	46	68	n/d	n/d
2d	n/d	n/d	n/d	15738	n/d	11083	128	2967	n/d	222	n/d	8	175	n/d	n/d	n/d
CTPs13	4993	14593	596	34642	n/d	3450	29	525	14	69	218	20	137	27	27	31
2a	2330	n/d	396	39503	n/a	601	30	n/d	8	67	n/a	19	451	38	n/a	n/a
3a	n/d	n/d	984	23572	n/a	5731	n/d	n/d	n/d	68	n/a	25	152	29	n/a	n/a
4a	n/d	n/d	807	40889	n/a	3376	28	n/d	n/d	70	n/a	8	78	n/d	n/a	n/a
5a	n/d	n/d	966	63937	n/a	4682	36	n/d	n/d	46	n/a	n/d	42	26	n/a	n/a
6a	n/d	n/d	1117	29621	n/a	3524	n/d	n/d	n/d	41	n/a	n/d	15	8	n/a	n/a
8a	7010	8418	n/d	71142	n/a	n/d	38	n/d	4	176	n/a	12	26	n/d	n/a	n/a
9a	3000	4713	120	15987	n/a	447	12	194	14	n/d	n/a	16	138	9	n/a	n/a
10a	4993	14635	596	9558	n/a	1600	24	913	n/d	n/d	n/a	46	118	n/d	n/a	n/a
11a	1985	25008	359	5499	n/a	n/d	21	681	37	342	n/a	13	2324	95	n/a	n/a
3c	12172	21809	374	64566	n/a	n/d	n/d	n/d	n/d	n/d	n/a	22	282	n/d	n/a	n/a
4c	5990	14842	2553	53306	n/a	n/d	n/d	46	n/d	n/d	n/a	n/d	224	n/d	n/a	n/a
5c	615	5591	561	34642	n/a	n/d	n/d	n/d	n/d	n/d	n/a	46	103	n/d	n/a	n/a
6c	1901	9157	665	74276	n/a	n/d	n/d	370	n/d	n/d	n/a	27	119	n/d	n/d	n/a
3d	16106	31337	n/d	23122	n/d	20074	327	8570	n/d	341	n/d	n/d	1507	77	27	46
4d	8742	14552	n/d	15372	n/d	n/d	n/d	n/d	14	n/d	218	27	137	33	n/d	16
CTPs2	2910	10731	3210	7874	n/d	8962	117	3081	86	10	251	28	45	11	13	8
5a	n/d	10731	1362	32707	n/a	n/d	n/d	n/d	n/d	n/d	n/a	37	n/d	n/d	n/a	n/a
6a	4394	11597	2606	7991	n/a	n/d	89	707	33	223	n/a	19	420	21	n/a	n/a
7a	1425	10977	2064	30203	n/a	6274	70	3081	103	41	n/a	n/d	45	n/d	n/a	n/a
8a	1038	14753	4998	1424	n/a	9273	117	3265	20	20	n/a	37	117	n/d	n/a	n/a
9a	n/d	7168	6918	7874	n/a	8650	154	2442	86	n/d	n/a	49	n/d	110	n/a	n/a
10a	n/d	6443	3826	3518	n/a	15427	n/d	3534	90	n/d	n/a	n/d	37	47	n/a	n/a
1d	774	545	n/d	324	n/d	n/d	5	n/d	n/d	9	n/d	1	4	1	1	n/d
2d	74097	26636	n/d	23525	n/d	n/d	126	n/d	n/d	519	n/d	n/d	17	n/d	57	16
3d	120590	10182	n/d	3489	n/d	n/d	182	n/d	n/d	160	251	52	62	n/d	13	n/d

[a] Numbers represent the sample point along the sample traverses (a–d). All data are in ppm; concentrations are normalized to 8600 ppm Al. n/a = not analyzed; n/d = not detected. Error on gas blank is 3 SD (σ).

monds and allows relative trace element enrichment/depletion patterns to be studied in the absence of an internal standard. No correction was made for matrix effects resulting from the higher ablation efficiency of diamond over the SRM glass. Griffin et al. (2004) and Dalphé and Ballantyne (2004) have shown that there is excellent agreement between results derived by calibration with carbon standards (cellulose and oil) and calibration using the NIST-612 glass, indicating that matrix effects are not too significant.

With this method of calculation, the analytical error on the concentration of each element is dependent on the absolute abundance of Al at a given ablation spot. The errors presented in Table 2 (core fluid data) and Table 3 (coat fluid data) are calculated using the average Al intensity in those regions; this gives higher errors for the core inclusions than the coat inclusions. The elemental detection limits are also a function of inclusion density at the ablation point, therefore an element may be below the detection limit because either it has a low concentration in the fluid, or the fluid inclusion density is low at the sampled point.

2.2.2. *FT-IR spectroscopy*

Infrared absorption spectra were recorded using a Vector22 Fourier-transformed infrared (FT-IR) spectrometer equipped with a HeNe laser (633 nm) and a Bruker IRScope-1 microscope at University College London. Spectra were recorded in transmission with a resolution of 4 cm^{-1} over the range 4000–650 cm^{-1}. The spot was 100 μm in diameter and was targeted over the laser ablation pits.

Lattice-bound nitrogen concentrations and aggregation states of the diamonds were calculated using the method of Mendelssohn and Milledge (1995). The lattice-bound nitrogen concentration of the diamond coats is highly variable (<20 to 1753 ppm) and nitrogen is present as nitrogen pairs (type IaA). All coat samples have a sharp absorption peak at 3107 cm^{-1}, which is commonly attributed to the presence of lattice bound hydrogen. All cores are aggregated type IaA-IaB with some platelet development. The concentrations of H_2O and CO_2 were calculated from the intensity of the O-H stretching band of water (using ε_{3420} = 80 L per mol cm^{-1}) and from the v_3 stretching band of carbonate (using ε_{1430} = 250 L per mol cm^{-1}); these values are used for consistency with previous studies (Navon et al., 1988; Schrauder et al., 1994; Zedgenizov et al., 2004). Since the absolute concentration of volatiles is dependent on inclusion density, we use the ratio $CO_2/(CO_2 + H_2O)$ to describe the volatile composition. Nitrogen and volatile characteristics of the coated diamonds are given in Table 1, along with included minerals detected in the FT-IR spectra of the diamond coat.

3. RESULTS

All elements in the diamond coats give higher counts than in the cores, this can be seen in the raw data plot (Fig. 1) and is a reflection of the higher inclusion density (therefore higher absolute element abundances). However, the level of enrichment in the coat over the core varies between elements: the intensities (in counts per second) of La, Sr and Ba are ≈20

Table 3. Median (shaded) trace element composition of diamond coat fluids and compositions of fluid at individual LA-ICP-MS sample spots (unshaded).[a]

Sample	Na	K	Sc	Ti	Mn	Fe	Co	Ni	Ga	Sr	Zr	Nb	Ba	La	Ta	U
error (3σ)	239	34	15	17	5	61	1.1	18	0.2	0.9	1	0.5	0.7	0.2	0.3	1
CTPb8	4543	22330	357	3268	n/d	12245	9	183	87	1877	156	45	5038	382	n/d	20
1a	1411	7418	818	2816	n/a	n/d	33	39	45	479	n/a	44	1646	100	n/a	n/a
2a	4524	16233	841	5792	n/a	n/d	9	231	76	2089	n/a	121	5689	434	n/a	n/a
3a	3039	12589	1259	3923	n/a	n/d	n/d	n/d	89	1877	n/a	134	3778	367	n/a	n/a
4a	5349	19517	524	4400	n/a	n/d	n/d	222	78	2591	n/a	110	5424	449	n/a	n/a
5a	4722	22330	769	3970	n/a	n/d	8	71	84	2328	n/a	43	5228	392	n/a	n/a
6a	2751	23230	191	2425	n/a	n/d	19	111	87	1915	n/a	12	5038	400	n/a	n/a
7a	2616	23232	333	3268	n/a	n/d	7	30	119	1787	n/a	14	6383	363	n/a	n/a
12a	4543	25493	181	2877	n/a	n/d	n/d	198	143	1993	n/a	35	7229	401	n/a	n/a
13a	7019	28231	222	3002	n/a	n/d	3	202	87	1850	n/a	25	4952	373	n/a	n/a
14a	5416	23514	357	2705	n/a	n/d	24	419	87	2172	n/a	51	4851	382	n/a	n/a
15a	5551	22478	354	5016	n/a	n/d	25	111	142	2779	n/a	73	5805	432	n/a	n/a
16a	5357	29139	755	4061	n/a	n/d	n/d	291	88	1658	n/a	63	3078	271	n/a	n/a
17a	2027	6521	466	831	n/a	n/d	5	168	34	584	n/a	45	1093	70	n/a	n/a
3d	n/d	19453	43	3540	n/d	14923	n/d	n/d	324	1849	216	45	6802	390	n/d	29
4d	n/d	5861	26	1805	n/d	9567	n/d	n/d	104	1146	96	25	2651	213	n/d	10
CTPs13	1511	17261	94	12182	147	5275	6	69	32	154	118	9	1781	100	8	4
1d	3434	5396	2	68990	214	1742	3	54	5	136	38	41	135	n/d	8	1
2d	1113	16921	8	3529	79	8808	6	78	125	281	198	7	2553	131	n/d	8
1a	2492	617	283	16264	n/a	n/d	10	10	24	212	n/a	12	1735	88	n/a	n/a
12a	1121	17601	30	4605	n/a	n/d	5	76	34	153	n/a	5	1840	101	n/a	n/a
1c	836	17911	37	3006	n/a	n/d	3	62	32	155	n/a	4	1846	99	n/a	n/a
2c	15342	38645	378	18896	n/a	n/d	n/d	8	31	149	n/a	20	1462	71	n/a	n/a
6c	1901	9157	665	74276	n/a	n/d	n/d	370	n/d	43	n/a	27	119	n/d	n/a	n/a
7c	835	20322	150	8100	n/a	n/d	6	126	36	219	n/a	7	1827	105	n/a	n/a
CTPs2	1948	15239	349	6450	n/d	11585	13	287	81	1815	197	44	4195	330	5	50
4d	7647	6659	n/d	19297	n/d	9621	96	n/d	159	1812	209	144	3932	251	5	49
5d	4431	13873	n/d	5955	n/d	13549	30	n/d	237	2820	184	99	6184	441	4	51
1a	n/d	11533	171	19111	n/a	n/d	n/d	937	n/d	911	n/a	40	1646	75	n/a	n/a
2a	1778	14450	n/d	2758	n/a	n/d	n/d	329	76	1578	n/a	28	4148	335	n/a	n/a
3a	1876	15546	5	13565	n/a	n/d	1	92	71	1363	n/a	16	4243	324	n/a	n/a
4a	174	11678	302	42005	n/a	n/d	n/d	323	18	815	n/a	48	2099	118	n/a	n/a
11a	2273	22380	321	6111	n/a	n/d	n/d	251	100	2086	n/a	7	6625	424	n/a	n/a
12a	2292	22109	349	3705	n/a	n/d	10	252	81	1929	n/a	23	5393	339	n/a	n/a
13a	1948	14931	520	3050	n/a	n/d	9	228	58	1818	n/a	73	3754	277	n/a	n/a
14a	1336	19261	654	3466	n/a	n/d	15	642	78	1731	n/a	78	3544	213	n/a	n/a
2c	n/d	52076	795	6789	n/a	n/d	n/d	n/d	266	4502	n/a	n/a	12513	873	n/a	n/a
9c	n/d	69658	3979	18042	n/a	n/d	n/d	n/d	461	8758	n/a	n/a	21585	1892	n/a	n/a
CTPs14	3221	17198	21	4113	n/d	10958	11	178	203	1597	391	14	4413	299	1	15
1a	2187	14813	21	2768	n/d	8412	19	180	317	1066	459	4	6738	222	1	22
2a	2824	17625	35	3794	n/d	11284	4	218	195	1638	391	12	4405	319	1	18
3a	3475	17403	53	5062	n/d	13529	n/d	188	230	1797	364	14	4584	375	1	26
4a	3414	16993	19	4474	n/d	11856	n/d	95	195	1613	392	18	4421	339	2	12
5a	3028	16326	2	4121	n/d	10088	n/d	176	202	1430	399	22	4264	279	n/d	9
6a	3618	17905	20	4106	n/d	10633	n/d	98	204	1581	280	15	4077	248	2	3
CDR3	2553	2467	38	3166	n/a	n/a	20	137	20	2699	n/a	86	7035	496	n/a	n/a
1a	1863	2198	38	2213	n/a	n/a	n/d	111	21	2286	n/a	86	5679	397	n/a	n/a
2a	2621	2702	n/d	3397	n/a	n/a	23	105	28	3194	n/a	145	8001	535	n/a	n/a
3a	2486	2231	n/d	2935	n/a	n/a	15	164	14	2505	n/a	78	6070	458	n/a	n/a
4a	3299	3063	n/d	3431	n/a	n/a	20	489	20	3526	n/a	85	8046	590	n/a	n/a

[a] Numbers represent the sample point along the sample traverses (a–d). All data are in ppm; concentrations are normalized to 8600 ppm Al. n/a = not analyzed; n/d = not detected. Error on gas blank is 3 SD (σ).

times higher in the coat than in those in the core; counts on K, Na and Al are ≈10 times higher; Ta, U and Zr are ≈4 times higher; Fe, Ga, Sc, Nb and Ti ≈10–15 times higher; and Ni and Co ≈3 times higher in the coat than in the core. Therefore, there are compositional differences between the fluid in inclusions in the diamond core and those in the coat.

The compositions of inclusions in the diamond cores (Fig. 2a) and coats (Fig. 2b) show a general 2–4-fold enrichment in incompatible elements (Ba, U, Nb, Ta, La, Sr, Zr) relative to major elements (Na, Al, Fe) when normalized to CI chondritic meteorites (McDonough and Sun, 1995). This high level of enrichment is unlikely to be due to the entrapment of mantle minerals and is more consistent with the presence of a fluid or quenched melt in the inclusions. Fesq et al. (1975) referred to such submicroscopic inclusions as "magma droplets." On cooling, minerals may precipitate from this quenched fluid (e.g., quartz, apatite and carbonate seen in the FT-IR spectra) and a trapped melt will quench to glass and may crystallize mineral phases, however this will not alter the bulk composition of the inclusions.

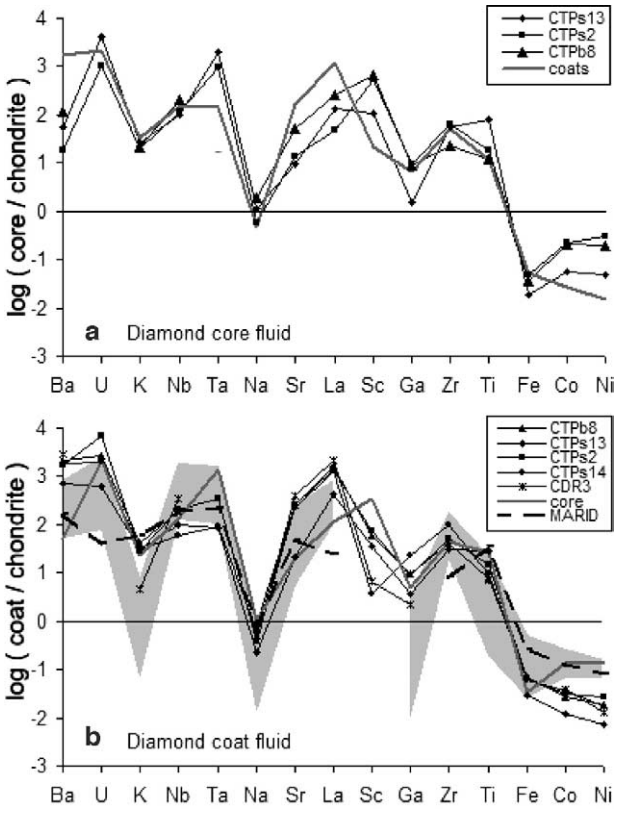

Fig. 2. Average trace element abundance patterns of diamond fluid normalized to carbonaceous chondrite (McDonough and Sun, 1995). (a) Average sample core fluids compositions (black lines) compared to average coat fluid (gray line). (b) Average composition of diamond sample coat fluids (black lines) and compositional range of kimberlite (shaded area; Dawson, 1980), MARID (heavy dashed line; Gregoire et al., 2002), and average core fluid composition (dark gray line). Sample symbols: CTPb8 (triangle), CTPs13 (diamond), CTPs2 (square), CTPs14 (circle), CDR3 (cross).

Nickel and cobalt have been detected as lattice impurities in synthetic diamonds grown from metal solvent catalysts at concentrations of <30 ppm and <1 ppm respectively (Hayakawa et al., 2000). Griffin et al. (2004) have determined absolute Ni and Co concentrations in fibrous diamond as 18.9 and 16.8 ppm respectively, using a carbon-based LA-ICP-MS standard. In this study we have only calculated the relative concentrations of trace elements in inclusions in the diamond, not the bulk diamond composition. However, lattice bound Ni and Co are not considered to be a significant component of the measured composition of the coated diamonds, because these elements are correlated with Fe in the core; Fe was not detected in the synthetic diamond lattice.

3.1. Diamond Core Fluids

The median compositions of the fluids in the diamond cores and the fluid data for individual analytical points are given in Table 2.

3.1.1. Incompatible elements

Inclusions in the diamond cores are generally enriched in high field strength elements (HFSE: Nb, Ta, Ti, Zr) over chondritic meteorites when Al-normalized (Fig. 2a): Ta by >3 orders of magnitude, Nb by >2 orders of magnitude and Zr and Ti by >1 order of magnitude. Although the Ta data are sparse, there appears to be a correlation between Ta and Ti, but not between Ti and Nb or Zr. HFSE enrichment may be due to the presence of rutile, titanates, sphene or ilmenite either as trapped crystalline phases or contributors to the glass/fluid. The diamond coat inclusions also contain very high concentrations of U, >3 times the concentration of U in chondritic meteorites for an equal Al content. This U-enrichment may be due to the influence of U-bearing minerals (apatite, zircon, monazite) either in as included minerals or constituents of the trapped glass/fluid; Zr may also be due to the presence of zircon. The other large ion lithophile elements (LILE: Ba, Sr, K) and La are enriched by 1 to 2 orders of magnitude over chondritic mantle (for the same Al content) in the diamond core fluid, the exception to this is Na which is present at approximately chondritic level (Fig. 2a). La, Ba and Sr are inter-correlated, but are not correlated with K or Na (Fig. 3a–c).

The enrichment of HFSE such as Ti, Zr and Ta in the diamond core fluid precludes carbonatite as the fluid trapped during diamond core growth, because carbonatite is typically low in HFSE (Ionov et al., 1993). When compared to natural carbonatite (Woolley and Kempe, 1989), La, Ba, Sr and Nb are depleted and the trace element pattern of the inclusions is different from that of carbonatite (Fig. 4). Therefore, we conclude that carbonatite-like fluid/melt was not important during core growth. This is relevant because carbonate-rich melts are commonly thought to be one of the main carbon sources and catalysts for diamond growth in the mantle and are the focus of diamond growth research in high-pressure high-temperature experiments (Akaishi et al., 1990; Litvin et al., 1998; Pal'yanov et al., 1999; Arima and Kozai, 2003).

Hydrous fluids are expected to show strong enrichment of highly soluble LILE (Sr, K, Ba) at the expense of insoluble HFSE (Ti, Zr, Nb, Ta). This is at odds with the observation that the diamond core fluids are enriched in HFSE relative to LILE. CO_2 reacts with silicate mantle minerals to form carbonate. Since there is no trace element evidence for carbonate involvement in the growth of the diamond cores, CO_2 is also not considered to be a dominant component of the diamond core fluid. This suggests that C-O-H fluids are unlikely to be the dominant fluid present in the diamond core inclusions.

High field strength element enrichment is often characteristic of silicate melt, while high Sr, Ba and Zr concentrations are expected in H_2O-rich silicate melts (Harte et al., 1993). Therefore, we favor a silicate melt (possibly hydrous) as the dominant component of the diamond core inclusions.

We have calculated the trace element compositions of mantle silicate minerals that would be in equilibrium with a silicate melt with the trace element composition of the diamond core fluids, normalized to 14 wt% Al_2O_3, using the partition coefficients of Klemme et al. (2002) and LaTourrette et al. (1995) (Table 4). The value of 14 wt% Al_2O_3 is the average Al concentration of the silicate melts generated during those partitioning experiments. The concentrations of most incompatible elements (K, Sr, Nb, Ba, La and U) are approximately within the range observed in natural mantle garnet and clinopyroxene and therefore concentration of these elements may have been generated locally by partial melting processes. However, the

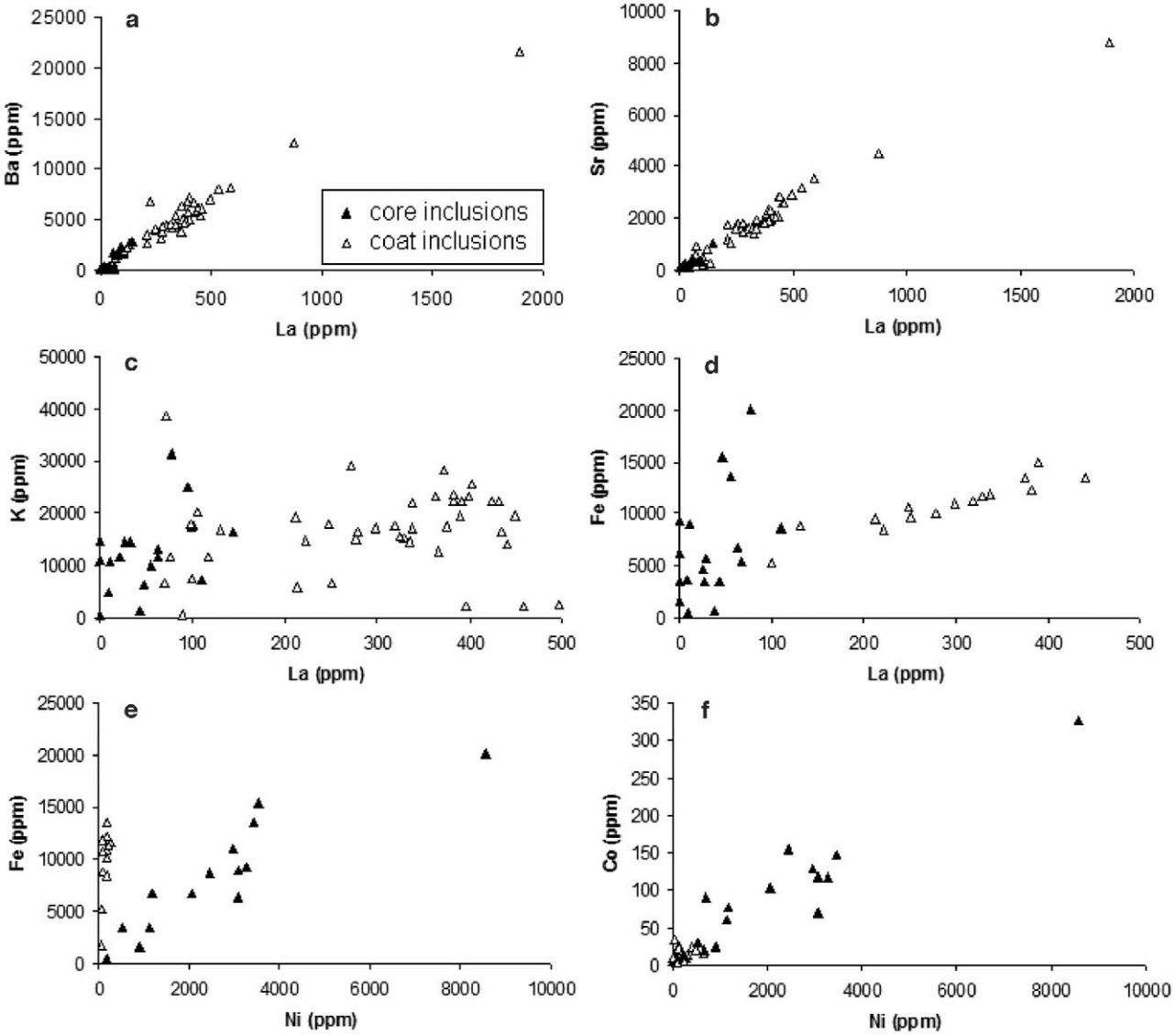

Fig. 3. Compositional variation of individual sample spots in diamond coat fluids (open triangles) and diamond core fluids (solid triangles). Concentrations are calculated relative to chondritic concentration of Al. (a) La and Ba are correlated in core and coat fluid; (b) La and Sr are correlated in core and coat fluid; (c) La and K are not correlated in either core or coat fluid; (d) La is correlated with Fe in coat but not in core fluid; (e) Ni and Fe are correlated in core fluid; (f) Ni and Co are correlated in core fluid.

calculated concentrations of Zr and Ti are very high and are therefore unlikely to have been generated by closed system partial melting of unmetasomatised mantle. The calculated range of incompatible element concentrations in phlogopite are significantly higher than observed in mantle samples, therefore phlogopite is unlikely to have been present at the time of diamond core growth.

3.1.2. *Compatible elements*

Diamond cores contain higher concentrations of compatible elements than their coats relative to chondritic Al. In the core region, Fe, Ni and Co are inter-correlated (Fig. 3e–f) and are depleted relative to chondritic meteorites for the same Al concentration (Fig. 2a). The Ni/Fe ratios of sample spots in the core range from 0.2 to 0.6, this is an order of magnitude higher than the average Ni/Fe ratio in peridotite-pyroxenite suite xenoliths (≈0.04) and two orders of magnitudes higher than in eclogite xenoliths (<0.001; calculated from Dawson, 1980). The ratios Ni/Co and Fe/Co are similarly high (≈23 and ≈78 respectively). We have calculated the concentration of Ni in olivine in equilibrium with a silicate melt with the average Ni concentration of the diamond core fluids normalized to 14 wt% Al_2O_3, using $D_{Ni}^{olivine/melt} = 10$ (Green, 1994). The calculated Ni concentration in olivine is 57,720 to 335,749 ppm, an order of magnitude higher than Ni in pyrolite mantle (1960 ppm Ni; McDonough and Sun, 1995) and in olivine diamond inclusions (2000 to 4000 ppm; Stachel et al., 2003). Therefore the high

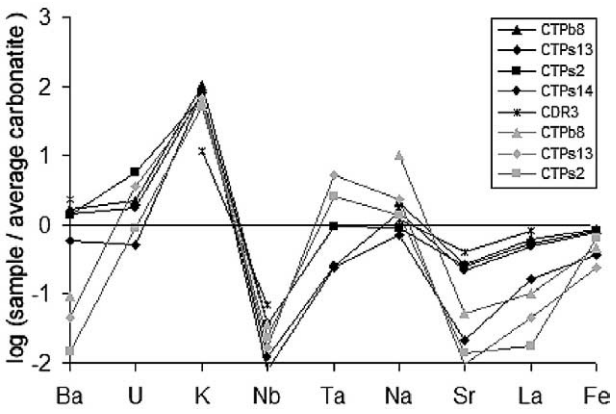

Fig. 4. Average composition of diamond coat fluids (black lines) and core fluids (gray lines) relative to chondritic Al, normalized to natural carbonatite (Woolley and Kempe, 1989). Sample symbols: CTPb8 (triangle), CTPs13 (diamond), CTPs2 (square), CTPs14 (circle), CDR3 (cross).

Ni/Fe and Co/Fe ratios may indicate the presence of a sulfide or metallic component in addition to the silicate melt in the diamond core inclusions. The trapped fluid has non-chondritic Ni/Fe and Ni/Co ratios, therefore the Ni and Co signature is unlikely to be due to metallic phases in the diamond cores. The Ni/Fe ratio of the diamond core inclusions (Ni/Fe = 0.2 to 0.6) are similar to those of sulfide inclusions in African diamonds (0–0.9; Deines and Harris, 1995).

In low pressure partitioning experiments between olivine and MORB melt, Li et al. (2003) found that Ni partition coefficients in S-bearing silicate systems were up to 50% lower than those derived from S-free experiments due to the formation of Ni-S complexes. Thompson and Barnes (1984) investigated the distribution of Ni and Fe between sulfides and olivine, and calculated a Ni/Fe partition coefficient of ≈9.8 ($KD^{sulfide/olivine}$ = sulfide X_{Ni}/X_{Fe}/Olivine X_{Ni}/X_{Fe}, where X denotes mole fractions). The calculated Ni/Fe ratio of olivine in equilibrium with a sulfide melt with the compatible element composition of the core fluid (Ni/Fe = 0.2 to 0.6) is 0.02 to 0.06, this is within the range observed for olivine inclusions in natural diamond (0.02–0.06; Hervig et al., 1980). Fleet and MacRae (1988) have determined this partition coefficient experimentally and give a higher value of ≈30, which they suggest is appropriate to the upper mantle. Using this higher value, olivine in equilibrium with the core fluid has a calculated Ni/Fe ratio of 0.007 to 0.02. Therefore, we suggest that Ni and Co in the trapped fluid/glass may be present as a sulfide phase.

Sulfide is the predominant diamond inclusion worldwide and is over abundant when compared to mantle peridotite and eclogite (Gurney, 1989). This study suggests that sulfide should also be expected as sub-microscopic inclusions, as is the case with glass and minerals (e.g., Fesq et al., 1975; Darmarupurshad et al., 1997). The presence of a sulfide component in silicate melt is not contrary to evidence from metasomatized xenoliths; sulfide minerals are common in eclogite xenoliths, often as inclusions in clinopyroxene and garnet (Taylor and Anand, 2004). Oxide-sulfide-silicate inclusion assemblages have been described in the centre of single diamonds from

Table 4. Calculated trace element compositions of silicate minerals in equilibrium with hydrous silicate melt with the average trace element composition of the diamond core fluids (normalized to 14 wt% Al_2O_3).[a]

Mineral	Sample	K	Na	Ti*	Ba	U	Nb	La	Sr	Zr*	Ta	Ni*
Diamond core fluid												
phl	CTPb8	383257	34976	60233	11083	—	42	19	667	17	—	—
	CTPs13	484470	8219	400100	5511	0.4	20	8	119	40	—	—
	CTPs2	356241	4790	90937	1800	0.09	27	3.3	174	47	—	—
cpx	CTPb8	881	—	20458	6	—	10	23	335	92	—	—
	CTPs13	1113	—	135891	2.8	2.7	5	10	60	220	3.5	—
	CTPs2	818	—	30886	0.9	0.7	6	4	88	255	2	—
grt	CTPb8	38	—	11934	0.12	—	3.8	0.5	21	394	—	—
	CTPs13	48	—	79270	0.06	2.0	1.8	0.2	3.8	948	1.2	—
	CTPs2	35	—	18017	0.02	0.5	2.4	0.09	5.5	1095	0.6	—
ol	CTPb8	—	—	—	—	—	—	—	—	—	—	225329
	CTPs13	—	—	—	—	—	—	—	—	—	—	57220
	CTPs2	—	—	—	—	—	—	—	—	—	—	335749
Observed mantle minerals												
phl[1]	Max	90071	3338	6165	470	0.4	15.5	0.6	30	20	1.6	1445
	Min	55205	223	1980	140	0.01	0.35	0.07	1.5	0.75	0.05	480
cpx[2]	Max	4068	31084	14564	19	—	1.49	8.91	200	20	—	—
	Min	332	5564	240	0.04	—	0.00	0.34	39.8	0.29	—	—
grt[2]	Max	0	2967	6833	3.22	—	8.52	0.74	31.3	176	—	—
	Min	0	668	14.2	0.00	—	0.00	0.00	0.12	1.54	—	—
ol[3]	Max	—	—	—	—	—	—	—	—	—	—	2000
	Min	—	—	—	—	—	—	—	—	—	—	4000

[a] Partition coefficients for core fluid calculation: phlogopite and amphibole from LaTourrette et al. (1995); clinopyroxene and garnet from Klemme et al. (2002); olivine from Green (1994) for hydrous silicate melts in equilibrium with basanite, eclogite, and peridotite, respectively. Concentrations are in ppm; elements marked with an asterisk are unreasonably high concentrations for mantle minerals. Observed mineral concentrations are from: 1, Gregoire et al. (2002); 2, Stachel et al. (2004); 3, Stachel et al. (2003). min = minimum; max = maximum; phl = phlogoptite; cpx = clinopyroxene; grt = garnet; ol = olivine.

Yakutia (Bulanova et al., 1998). Therefore, we favor a silicate-sulfide melt as the fluid present in submicroscopic inclusions in the diamond core.

3.1.3. Paragenesis

The Ni/Fe ratios of the trapped sulfide give a FeNiS sulfide phase with 8 to 27 mol% Ni, this is intermediate between the Ni content of peridotitic (>12%) and eclogitic (<12%) sulfides (Deines and Harris, 1995), so it is not possible to assign a paragenesis to the diamond cores on the basis of inferred sulfide composition. Rege et al. (2003) showed that eclogitic and super-deep diamonds typically have negative HFSE (Nb, Zr, Ti) anomalies, while peridotitic diamonds from different global locations show variable degrees of HFSE enrichment. The ratio Nb/La in the diamond core fluid is ≈ 0.8, this is similar to the Nb/La ratio in peridotitic diamonds from global locations (Nb/La ≈ 0.66 in peridotitic diamonds, Nb/La ≈ 0.02 eclogitic diamonds, calculated from Rege et al. (2003). This suggests that the diamond cores in this study may be peridotitic.

3.2. Diamond Coat Fluids

The median compositions of the diamond coat fluids and the data for individual analytical points are given in Table 3. Inclusions in the diamond coat are enriched in La, Ba and Sr and depleted in Ta, Ti, Sc, Ni and Co relative to the diamond core fluids when the data are Al-normalized. Relative to Al, the concentrations of the other incompatible elements (U, K, Nb, Na, Ga, Zr) and Fe are approximately equal in both the diamond core and coat fluids.

3.2.1. Incompatible elements

When normalized to CI chondrites and baselined to chondritic Al, Na is present at approximately chondritic concentrations; the remaining LILE and La are enriched by approximately 1.5 to 3.3 orders of magnitude, increasing in the order K<Sr<La<Ba<U (Fig. 2b). There is a positive correlation between La, Ba, Sr and Fe in the diamond coat inclusions (Fig. 3a–c). The chondrite normalized trace element pattern is similar to that of fibrous diamonds from Botswana (Schrauder et al., 1996), Canada and Siberia (Griffin et al., 2004).

The HFSE (Ta, Nb, Zr) concentrations of the extrapolated diamond coat fluids are enriched by a factor of ≈2 over CI chondrites; Ti is only moderately enriched relative to chondritic Al. The HFSE ratios in the diamond coat fluids are generally similar to those in the diamond core inclusions, the ratio Nb/Zr ranges from 0.04 to 0.29 in the coat (mean 0.16), in the core the range is 0.09 to 0.48 (mean 0.23); Zr/Ti = 0.01 to 0.1 (mean 0.02) in the coat inclusions and 0.01 to 0.03 (mean 0.02) in the diamond core inclusions. The elements K, Na and U are also present in similar ratios in the coat fluid as in the core fluid: Zr/K = 0.007 to 0.023 (0.008 to 0.023 in the diamond core fluid); Nb/Na = 0.005 to 0.024 (0.004 to 0.013 in the diamond core fluid). Therefore, the fluid trapped in inclusions in the diamond coat may contain a component of silicate melt similar to that in the diamond core inclusions. The presence of a hydrous silicate fluid component is consistent with H_2O and quartz in the infrared spectra of the diamond coats (Table 1).

The main difference between the diamond core fluid and that trapped in inclusions in the diamond coat appears to be the LILE- and La-enrichment of the latter. In Figure 4 we compare the Al-normalized LILE plus La, Fe Nb and Ta composition of the diamond coat fluids to natural carbonatite (data from Woolley and Kempe, 1989); these elements are commonly enriched in carbonatite. Most elements deviate by less than one order of magnitude from the carbonatite axis, the exception to this is K, which is enriched by two orders of magnitude over natural carbonatite and Nb which is depleted by two orders of magnitude (Fig. 4). The similarity between the coat fluid and carbonatite may be expressed by ratios Na/Ba ≈0.66, La/Ta≈130 (0.71 and 122, respectively, in carbonatite; Woolley and Kempe, 1989). This is the case even for samples with no detectable carbonate or CO_2 in the FT-IR spectra (Table 1). The Nb depletion of the coat fluid relative to carbonatite may reflect competition for Nb, for example with rutile. The high K-content relative to the other LILE may be due to the presence of a K-rich mineral such as phlogopite, or due to a component of KCl brine in the inclusions. The presence of KCl has been detected in individual fluid inclusions in fibrous diamonds from Canada by EMPA (Klein-BenDavid et al., 2002), while fibrous diamonds from Botswana (Schrauder and Navon, 1994) contain detectable concentrations of Cl, which shows a positive correlation with K. Furthermore, studies of the noble gas and halogen geochemistry of fibrous diamond fluids have also reveal high and correlated K and Cl contents (18–59 and 6–19 ppm respectively) in diamonds from the DRC (Johnson et al., 2000). Brine may be an evolved form of carbonatitic fluid formed by crystallization of mantle phases.

Therefore, we suggest that the diamond coats contain inclusions of carbonatite-like fluid and a component of hydrous-silicate melt similar to that in the diamond core inclusions. Silicate and carbonatitic fluid end-members have previously been identified in fluid inclusions in fibrous diamonds from the DRC and Botswana (Navon et al., 1988; Schrauder et al., 1996). Schrauder et al. (1996) show that incompatible element concentrations are a factor of two higher in the carbonatitic end-member than in the silicate fluid.

The overall normalized trace element pattern of the diamond coat inclusions is broadly similar to that of group I kimberlite (Fig. 2b); the diamond coat fluid ratios of Nb/Zr = 0.04 to 0.29 and Nb/Ta = 7.9 to 11.3 are within the kimberlite range. The similarity to kimberlite has been noted previously (Akagi and Masuda, 1988; Schrauder et al., 1996; Griffin et al., 2004). However, there are important differences; the trapped fluid is more enriched in LILE (Ba, K, U, Sr,) and La and is relatively depleted in HFSE (Nb, Ta, Ti and to a lesser extent Zr) when baselined to chondritic-Al. This is demonstrated by comparing trace element ratios in the diamond coat to those from the Mbuji Mayi kimberlite, the host kimberlite for these samples The diamond coat has Nb/Ba = 0.003 to 0.012 and Nb/La = 0.05 to 0.17, which are an order or magnitude lower than in the Mbuji Mayi kimberlite (Nb/La = 0.45 ± 0.25, Nb/La = 3.0 ± 1.1; data from Fieremans et al., 1984; Taylor et al., 1994); Ta/K = 0.0001 to 0.0003 and Ta/U = 0.086 to 0.26, also order of magnitude lower than the Mbuji Mayi kimberlite (Ta/K = 0.004 ± 0.003, Ta/U = 4.5 ± 3, data from Fieremans et al., 1984; Taylor et al., 1994).

The chondrite-normalized trace element pattern of the dia-

mond coat inclusions is also similar to MARID (mica-amphibole-rutile-ilmenite-diopside), the main difference being the higher relative concentrations of Ba, Sr and La in the diamond coat inclusions (Fig. 2b). Gregoire et al. (2002) proposed that MARID is a highly alkaline melt genetically linked to Group II kimberlite, which percolated through and metasomatized the upper mantle (Jones, 1989). Therefore, MARID may be a relevant melt/fluid source for the fluid trapped as inclusions in the diamond coats. PIC (phlogopite-ilmenite-clinopyroxene) is the Group I kimberlite equivalent of MARID (Gregoire et al., 2002) and therefore may be more relevant to fibrous diamond growth, because coated diamonds are only known from group I kimberlites (Boyd et al., 1992).

3.2.2. Compatible elements

Concentrations of compatible elements (Fe, Ni, Co) in the diamond coat fluid are depleted relative to CI chondrites for a given Al concentration (Fig. 2b). While the concentration of Fe in the diamond cores is correlated with Ni and Co and is attributed to the presence of sulfide, this is not the case in the diamond coats. Iron is generally positively correlated with the LIL elements in the diamond coats and is associated with the carbonatite component (this may mask any contribution from Fe-sulfides). The average sample Ni/Co ratio is ≈16 (range 7 to 23), this is lower than in the diamond cores where Ni/Co ≈ 23. The Ni concentration of olivine in equilibrium with a carbonate melt with the Ni-content of the diamond coat fluid (calculated using $D_{Ni}^{olivine/melt} = 19.1$; from Sweeney et al., 1995), varies between 1323 and 5490 ppm (average 3268 ppm). This largely overlaps with the range of Ni concentrations in olivine diamond inclusions is 2000 to 4000 ppm (Stachel et al., 2003), so Ni may reside in the carbonate melt in the diamond coat inclusions.

3.3. Zoning

The diamond cores do not show systematic zoning in fluid composition. Trace element zoning was not expected because all of the cores show evidence for growth during more than one event, however zoning is also not apparent within single growth zones (e.g., in sample CTPs13 the traverse sampled several points within a single growth zone, Fig. 5). Fluid inclusions appear to be compositionally zoned in the diamond coats. In sample CTPs13 (Fig. 5) and CDR3 inclusions become more enriched in carbonatite components (Ba, La, Sr) towards the rim, relative to Al; Nb initially increases then decreases perhaps reflecting competition of Nb between accessory silicate minerals (e.g., rutile) and carbonatite. In CTPb8, CTPs14 and CTPs2 (Fig. 5) the carbonatite components initially increase away from the core-coat boundary, then decrease reflecting an increase in the relative concentration of Al towards the rim. Therefore, the diamond coats seem to record changes in the fluid composition during fibrous diamond growth, but the change is not consistently towards more LIL element- or HFSE-rich fluid.

4. DISCUSSION

4.1. Diamond Core Fluid Formation

The single crystal morphology of the diamond cores indicates that growth rates during crystallization of the cores were lower than during formation of their coats and that the system was saturated (but not supersaturated) in carbon. This may be due to lower volatile concentrations and/or differences in carbon speciation relative to the diamond coat growth period. The core fluids are characterized by strong enrichment of all incompatible elements, in particular the HFSE (Ti, Ta, Zr, Nb), U and K relative to Al. This is consistent with the entrapment of silicate and sulfide melts. Generating 2–4-fold enrichment across the incompatible element spectrum by partial melting in the diamond stability field is unlikely; such enrichment is more easily achieved by fractionation of silicate melt or by the infiltration of a metasomatic fluid. These models will be considered below.

4.1.1. Igneous core growth

Bulanova et al. (1995) suggested that diamond may crystallize from a fractionating silicate-sulfide melt. This model is consistent with the high concentration of transition elements in diamond cores. The solubility of carbon in sulfide melts is an order of magnitude higher than in silicate melts (Saxena, 1989). Therefore, this model provides a means of saturating the growth environment in carbon. The concentrations of Ti, Zr and K in the fluid/glass inclusions in the diamond cores are too high to be in equilibrium with a mantle silicate assemblage, however the fluid may be shielded from mantle minerals by earlier fluid precipitates. The fractional crystallization model is inconsistent with the lack of systematic trace element trends across growth zones in the diamond cores. Therefore, there is no clear signal that the diamond cores grew during igneous fractionation.

4.1.2. Metasomatic core growth

Fluids and melts percolating through the mantle are a potential source of both incompatible elements and carbon. Migrating fluids are heterogeneous because they may only achieve equilibrium on a very local scale, which means that fluid compositions may vary within single growth zone. Single gem diamonds, comparable to the diamond cores, may record the full range of $\delta^{13}C$ isotopic variability observed in bulk analyses of individual diamonds (Hauri et al., 2002). The high Zr and Ti concentrations of the diamond core fluids may suggest an open system during diamond core growth. These elements may be supplied by a metasomatizing silicate melt. Infiltration of silicate melts into subsolidus peridotite requires H_2O-rich compositions to prevent the melt from crystallizing and stagnating (Stachel and Harris, 1997). The introduction of this fluid lowers the mantle solidus temperature, dissolves aluminosilicate components from the wall rock minerals, and may lead to partial melting. Diamond may crystallize directly from the metasomatic fluid, or from these partial melts, or from a reaction product of the two. Almost all eclogites from the Yakutian kimberlites show evidence of having experienced partial melting (e.g., spongy clinopyroxene, kelphytic rims on garnet and K-rich aluminosilicate glass; Spetsius, 1995). Phlogopite is not thought to have formed during this metasomatic event, as it would not be in equilibrium with the trace element composition of the silicate melt.

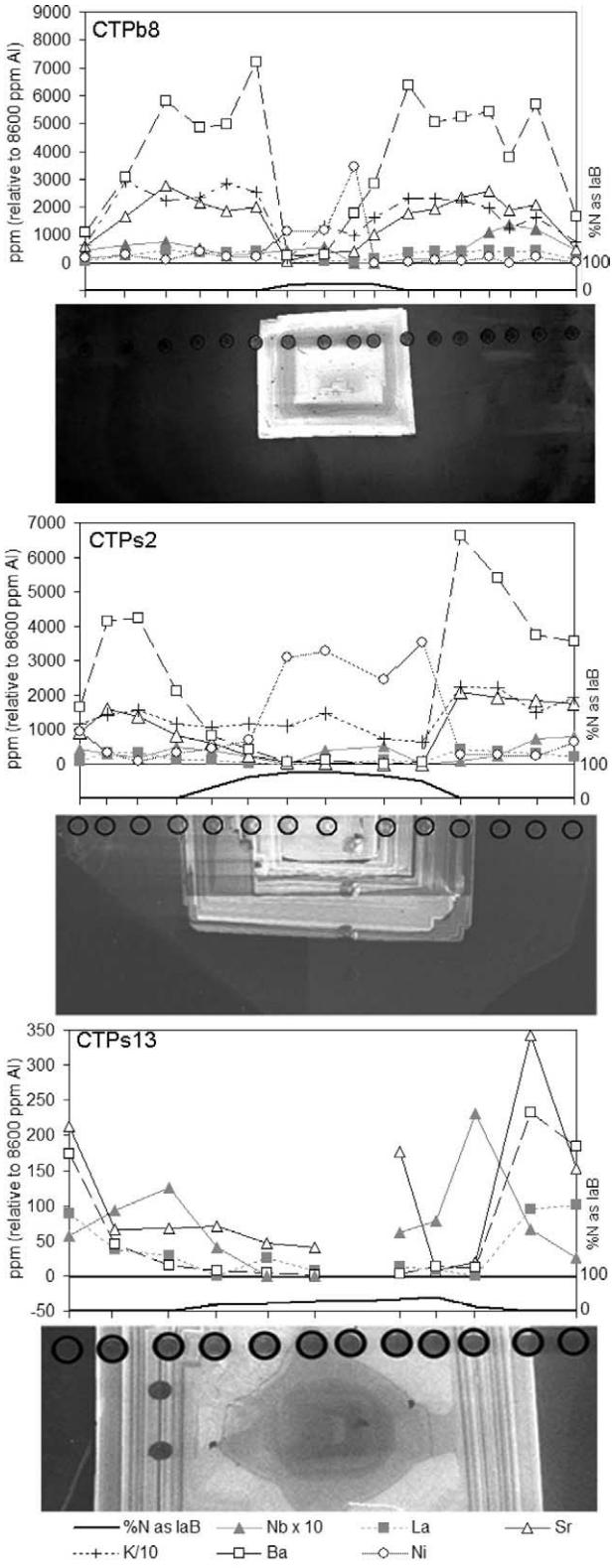

Fig. 5. Inclusion compositions along traverse through coated diamonds and cathodoluminescence image showing sample points and internal zoning along traverse (circled). Left axis shows trace element compositions; right axis shows nitrogen aggregation. Concentrations as in key except CTPs13 shows Ba/10 and Nb × 5 (not Ba and Nb × 10). No data are available for CTPs13 point 7 because Al was below detection limit.

4.2. Diamond Coat Fluid Formation

The symmetrical and fibrous morphology and the presence of volatile-filled cavities in the diamond coats indicate rapid diamond growth under conditions of fluid and carbon supersaturation. This situation may be achieved by diamond growth in a carbonatitic fluid. The striking morphological difference between cores and the coats, and the difference in age recorded by the nitrogen aggregation state in these samples, argue in favor of a 2-stage process for the growth of coated diamond. The overall similarity of the HFSE, K and Na ratios of the diamond core and coat fluids allows that both parts grew in the presence of similar fluid, we suggest that this fluid was silicate melt.

In addition to the silicate melt, the diamond coat inclusions contain varying quantities of a carbonatite-like component. This is expressed as enrichment in Ba, Sr and La relative to the core fluid (normalized the same Al-concentration). The presence of this carbonate component may be explained by two models: (1) carbonate influx and metasomatism of the preenriched mantle, and (2) low degree partial melting of the preenriched mantle, as proposed by Schrauder et al. (1996). The composition of silicate melt generated during both of these processes will be modified by partial melting, dissolution and alteration of accessory and mantle minerals that were formed during previous metasomatic events, possibly including the event(s) during which the core of the diamond formed.

4.2.1. *Carbonate influx and fractional crystallization*

An influx of carbonate into the pre-enriched peridotite or eclogite mantle would introduce additional LILE. In-situ crystallization of carbonates and apatite (as seen in the FT-IR spectra of the diamond coats) would then drive the fluid towards a more silicate-rich composition. The different zoning patterns observed in the diamond coats may reflect the timing of diamond growth in relation to fractionation. This model assumes that the carbon source for diamond coat growth was different from that for diamond core growth and so is in agreement with the general observation that fibrous diamonds have restricted and globally uniform range of $\delta^{13}C$ values of -5 to $-8‰$ (Boyd et al., 1992). This model is in agreement with the dominance of H_2O over CO_2 ($CO_2/(CO_2 + H_2O) < 0.4$) in the coat, as the precipitation of carbonate minerals will drive the remaining fluid composition towards more H_2O-rich compositions. However, carbonate influx may also initiate dehydration and partial melting of metasomatic (including hydrous and nominally anhydrous) phases formed during previous metasomatic events. In this scenario, the trapped fluid represents a reaction product between the mantle assemblage and the infiltrating carbonatitic metasomatic agent.

4.2.2. *Partial melting of enriched mantle*

Dalton and Presnall (1998) and Moore and Wood (1998) demonstrated that solidus melting of carbonated lherzolite within the diamond stability field (3–7 GPa) produces carbonatite melts. In similar experiments using carbonated eclogite, Yaxley and Brey (2004) show that solidus (1310°C at 5 GPa) and low degree (<0.3%) partial melting of carbonate-bearing eclogite also produces carbonate melts. The eclogite melts are markedly more calcic than those produced during melting of

carbonated peridotite. Ryabchikov et al. (1991) showed that carbonate melts generated near the peridotite solidus can dissolve appreciable amounts of apatite (up to 10 wt% P_2O_5), this can explain the presence of apatite in the FT-IR spectra of diamond coats. Low degree partial melting of the preenriched host may generate Ba, Sr, La and U-bearing volatile-rich fluids. In this scenario, the trapped fluid represents an in-situ melt generated from preexisting metasomatic phases. The zoning patterns recorded in individual diamond coats would depend on the phases present in the local growth region.

The main argument against this model is the global uniformity in the range of $\delta^{13}C$ values for fibrous diamond. Carbon introduced during the diamond core-forming event and later released by local partial melting for diamond coat formation, should form a coat with a similar isotopic composition as the core, unless $\delta^{13}C$ is fractionated during partial melting of carbonate or by the separation of a CO_2-rich fluid from the carbonate melt. This model also requires a change in pressure and/or temperature to initiate melting by decompression, dehydration or at the solidus. Alternatively, melting may be initiated by the injection of a fluid (e.g., from a plume, subducted slab, or leaked from mantle convection cells). This fluid may supply carbon for diamond growth. An influx of C-O-H fluid is supported by the high concentrations of H_2O and CO_2 determined from the infrared spectra of the diamond coats. With increasing degrees of partial melting, the experimental lherzolite and eclogite melts of Dalton and Presnell (1998) and Yaxley and Brey (2004), respectively, evolve smoothly from carbonate-rich to silicate-rich melts similar to kimberlite (at ≈1 % partial melting).

4.2.3. Comparison between coat fluid and kimberlite melt

Akagi and Masuda (1988) used the similarity between the $^{87}Sr/^{86}Sr$ ratios (0.7038–0.7252) of fibrous diamonds from Mbuji Mayi and the Mbui Mayi kimberlite magma, to suggest that fluid inclusions in fibrous diamonds were trapped as the diamond grew, either in the kimberlite melt, or in the kimberlite source. This is supported by the similarity between the $\delta^{13}C$ composition of fibrous diamond and that of carbonate in kimberlite (Kirkley et al., 1989). However, inclusions in fibrous diamonds retain a residual internal pressure of 1.4 to 2.0 GPa, corresponding to a formation pressure of 4–7 GPa (Navon, 1991), so these fibrous diamonds must have grown at depth rather than during kimberlite ascent. Phenocrystic growth of fibrous diamond is also not consistent with the composition of the trapped fluids (high LILE concentrations, Ti-rich) or with the ubiquitous IaA nitrogen aggregation state of fibrous diamond, which requires the diamond to be resident in the mantle for a period of time (albeit short) prior to kimberlite eruption (Boyd et al., 1994). Therefore, fibrous diamond is a xenocryst in kimberlite magma (Boyd et al., 1987). However, the diamond coat may have grown in the kimberlite source region during the early stages of kimberlite melt generation, or from a fluid separated from kimberlite melt.

In order to evaluate whether the fluid/melt trapped in the coat is related to the kimberlite source, we have compared the incompatible element composition of the fluid in the diamond coat with that of unaltered kimberlite from Koidu, Sierra Leone (data from Taylor et al., 1994). Koidu was chosen, in the absence of complete trace element data from Mbuji Mayi, because it is a group I kimberlite. If the trapped fluid is genetically related to kimberlite, then kimberlite should lie along an extension of the compositional trend of the diamond coat inclusions in the ternary diagrams in Figure 6. This is true for Sr-Ba-La (Fig. 6a), for which there is an overlap between the fluid composition and that of the Koidu kimberlite, the main difference being the stronger Ba enrichment of the fluid in the diamond coats. The relationship is also true for Nb-Ti-K (Fig. 6b); here the trapped fluid contains a higher concentration of K,

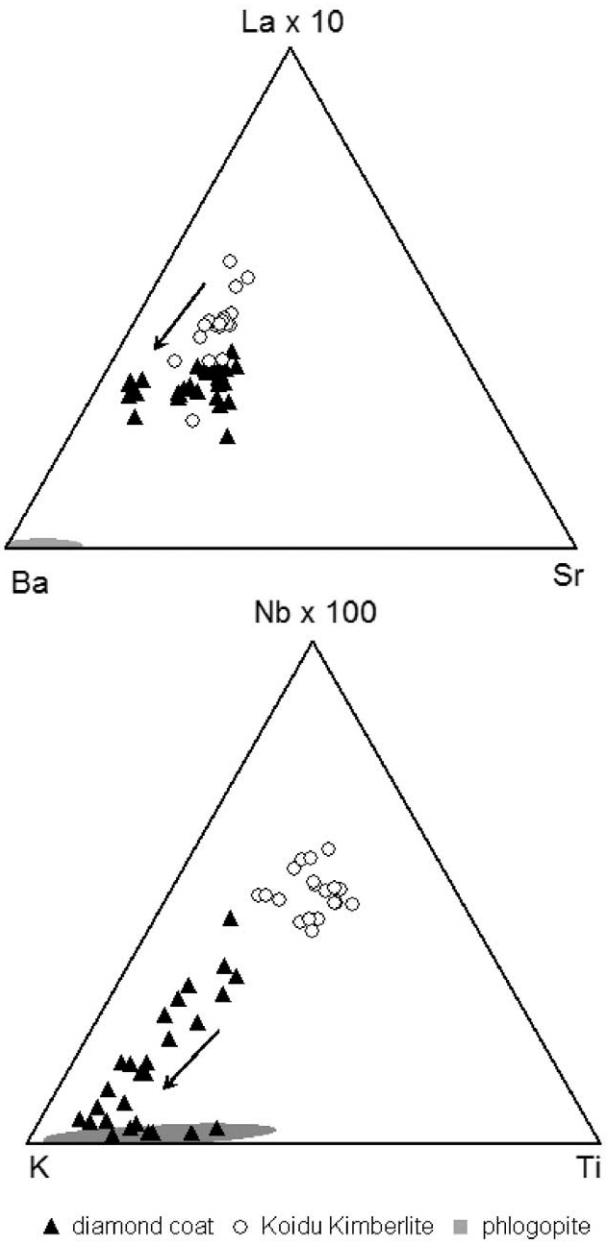

Fig. 6. Ternary diagram showing incompatible element concentrations in diamond coat fluids (black triangles) compared to composition of Koidu group I kimberlite (open circles; data from Taylor et al., 1994). (a) La-Ba-Sr; (b) Nb-K-Ti. Phlogopite field is shown in gray. Kimberlite may be obtained by crystallizing phlogopite from trapped fluid in diamond coats.

resulting in lower element/K ratios for the fluid than for kimberlite. Therefore, much of the trace element composition of the diamond coat fluid in these samples is consistent with a genetic relationship with the kimberlite source. This implies a possible relationship between fibrous diamond growth and kimberlite petrogenesis.

The composition of the Koidu kimberlite may be obtained by crystallizing phlogopite from the fluid/melt trapped in the diamond coat, for example by metasomatic reaction with the wall rock. This may lead to the formation of phlogopite-rich and PIC suite mantle rocks (Gregoire et al., 2002), which later become entrained in ascending kimberlite melt. Alternatively, K-concentrations in the fluid may also be reduced by the formation and separation of a KCl fluid similar to the brine described in cloudy diamonds (Izraeli et al., 2001).

5. CONCLUSIONS

Coated diamonds allow investigation of the environment and process of both octahedral and fibrous diamond growth. Both the diamond core and coat inclusions show a general 2–4-fold enrichment in incompatible elements relative to Al. This strong enrichment is unlikely to be due to the entrapment of silicate mantle minerals (olivine, garnet, clinopyroxene, phlogopite) alone and we infer the presence of sub-microscopic fluid or glass inclusions in both regions. The diamond core fluids are strongly enriched in HFSE (Nb, Ti, Ta, Zr) and U relative to Al, and moderately enriched in LILE (Ba, Sr, K). This fluid is not likely to be carbonatitic, but the trace element composition is consistent with the trapped fluid being a silicate melt. We favor a model in which incompatible element enrichment is achieved by the introduction of a metasomatic silicate fluid/melt and the diamond cores crystallized either directly from this metasomatic fluid or from the reaction product of interaction between the incoming melt and the host mantle. However, the Ni content and Ni/Fe ratio of the trapped fluid are very high for a silicate melt in equilibrium with mantle minerals; the Ni and Co signature of the diamond core fluid is thought to be dominated by a sulfide phase. In contrast, the diamond coats grew in the presence of a fluid that is strongly enriched in LILE (U, Ba, Sr, K) and La, and only moderately enriched in HFSE (Ta, Nb, Zr) when normalized to chondritic Al. LILE and La enrichment is interpreted as due to the presence of a carbonatitic fluid in the diamond coat inclusions, which is mixed with a HFSE-rich hydrous silicate fluid similar to that in the core. Much of the composition of the coat fluid is consistent with a genetic link to group 1 kimberlite.

The cores and coats of the coated diamonds in this study grew from different types of fluid, which is consistent with the observation that cores and coats in similar diamonds to those studied here have distinctly different $\delta^{13}C$ and $\delta^{15}N$ compositions (Boyd et al., 1992). Since the fluid medium is likely to be the solvent-catalyst for diamond growth, the difference in growth mode may be a result of this difference in the nature of the fluid. Silicate-sulfide melt is one of a number of possible growth fluids for gem diamonds. Carbonate is ubiquitously present in fibrous diamonds from Africa, Siberia and Canada (Navon et al., 1988; Guthrie et al., 1991; Schrauder and Navon, 1994; Klein-BenDavid et al., 2002; Zedgenizov et al., 2004).

Laser Ablation ICP-MS is valuable tool for determining the composition and variability of very low level (ppm to ppb) impurities included in diamond. The "chemically transparent" nature of diamond allows direct observation of the mantle melts present during diamond growth. The use of relative concentrations enables the trace element enrichment and depletion patterns of diamond inclusions to be studied in the absence of an internal standard. This has led to the recognition of discrete signatures that we have interpreted in terms of various proportions of silicate, sulfide and carbonatite melts in coated diamonds from the DRC. Awareness of the types of fluids that are involved in diamond growth is important for understanding diamond growth and interpreting the wide variability of diamond trace element compositions (e.g., Rege et al., 2003). Information about the relative importance of various fluid types during diamond growth at different localities can provide the basis for statistical "fingerprinting" of diamonds (Resano et al., 2003; De Corte et al., 2004).

Acknowledgments—This research is funded by an EPSRC Industrial CASE studentship (01302499) with DeBeers Industrial Diamonds. Dr. Andy Beard and Prof. Judith Milledge are thanked for help with the EMPA and for advice on this text. Also Prof. Hilary Downs for useful comments on this manuscript Dr. James Shigley is thanked for providing sample CDR3. Thanks also to Jacques Jones and Andy Taylor of the Diamond Trading Company (DTC) for sample cutting and polishing. Prof. Bill Griffin and an anonymous reviewer are thanked for providing valuable feedback in review.

Associate editor: C. R. Neal

REFERENCES

Akagi T. and Masuda A. (1988) Isotopic and elemental evidence for a relationship between kimberlite and zaire cubic diamonds. *Nature* **336** (*6200*), 665–667.

Akaishi M., Kanda H., and Yamaoka S. (1990) Synthesis of diamond from graphite-carbonate systems under very high temperature and pressure. *J. Crystal Growth* **104,** 578–581.

Arima M. and Kozai Y. (2003) Diamond crystallization from carbonatitic melts by metasomatic reducing reactions. *Geochim. Cosmochim. Acta* **67,** A23–A23.

Bibby D. M. (1982) Impurities in natural diamond. *Chem. Phys. Carbon* **18,** 3–91.

Boyd S. R., Mattey D. P., Pillinger C. T., Milledge H. J., Mendelssohn M. J., and Seal M. (1987) Multiple growth events during diamond genesis: An integrated study of carbon and nitrogen isotopes and nitrogen aggregation state in coated stones. *Earth Planet. Sci. Lett.* **86,** 341–353.

Boyd S. R., Pillinger C. T., Milledge H. J., and Seal M. J. (1992) C-isotopic and N-isotopic composition and the infrared-absorption spectra of coated diamonds—Evidence for the regional uniformity of CO_2-H_2O rich fluids in lithospheric mantle. *Earth Planet. Sci. Lett.* **108,** 139–150.

Boyd S. R., Pineau F., and Javoy M. (1994) Modeling the growth of natural diamonds. *Chem. Geol.* **116,** 29–42.

Bulanova G. P. (1995) The formation of diamond. *J. Geochem. Explor.* **53,** 1–23.

Bulanova G. P., Griffin W. L., and Ryan C. G. (1998) Nucleation environment of diamonds from Yakutian kimberlites. *Min. Mag.* **62,** 409–419.

Cartigny P., Harris J. W., and Javoy M. (2001) Diamond genesis, mantle fractionations and mantle nitrogen content: A study of $\delta^{13}C$-N concentrations in diamonds. *Earth Planet. Sci. Lett.* **185,** 85–98.

Dalphé C. and Ballantyne D. J. (2004) Quantitative analysis of ultra-trace impurities in carbon-based materials by LA-ICP-MS: Application to diamond profiling. In *Proceedings of the 55th Diamond Conference,* pp. 7.1–7.2.

Dalton J. A. and Presnall D. C. (1998) Carbonatitic melts along the solidus of model lherzolite in the system CaO-MgO-Al_2O_3-SiO_2-CO_2 from 3 to 7 GPa. *Contrib. Mineral. Petrol.* **131,** 123–135.

Damarupurshad A., Hart R. J., Sellschop J. P. F., and Meyer H. O. A. (1997) The application of INAA to the geochemical analysis of single diamonds. *J. Radioanalyt. Nucl. Chem.* **219,** 33–39.

Dawson J. B. (1980) *Kimberlites and Their Xenoliths.* Springer-Verlag.

De Corte K., De Schrijver I., Vanhaecke F., and Moens L. (2004) Is there a correlation between the chemical fingerprint of gem diamonds from a single mine and their nitrogen content or paragenesis? An LA-ICP-MS case study of diamonds from Premier (South Africa), De Beers Pool (South Africa) and Udachnaya (Russia). In *Proceedings of the 55th Diamond Conference,* p. 8.1.

Deines P. and Harris J. W. (1995) Sulfide inclusion chemistry and carbon isotopes of African diamonds. *Geochim. Cosmochim. Acta* **59,** 3173–3188.

Deines P., Viljoen F., and Harris J. W. (2001) Implications of the carbon isotope and mineral inclusion record for the formation of diamonds in the mantle underlying a mobile belt: Venetia, South Africa. *Geochim. Cosmochim. Acta* **65,** 813–838.

Fesq H. W., Bibby D. M., Erasmus C. S., Kable E. J. D. and Sellschop J. P. F. (1975) Determination of trace element impurities in natural diamonds by instrumental neutron activation analysis. In *Physics and Chemistry of the Earth*, Vol. 9 (eds. L. H. Aherns, J. B. Dawson, A. R. Duncan and A. J. Erlank), p. 817–836. Pergamon Press.

Fieremans J., Hertogen J. and Demaiffe D. (1984) Petrology, geochemistry and strontium isotopic composition of the Mbuji Mayi and Kundelungu kimberlites (Zaire). In *Kimberlites, I: Kimberlites and Related Rocks* (ed. J. Kornprobst), pp. 107–120. Elsevier Science.

Fleet M. E. and MacRae N. D. (1988) Partition of Ni between olivine and sulfide—Equilibria with sulfide-oxide liquids. *Contrib. Mineral. Petrol.* **100,** 462–469.

Green T. H. (1994) Experimental studies of trace-element partitioning applicable to igneous petrogenesis—Sedona 16 years later. *Chem. Geol.* **117,** 1–36.

Gregoire M., Bell D. R., and Le Roex A. P. (2002) Trace element geochemistry of phlogopite-rich mafic mantle xenoliths: Their classification and their relationship to phlogopite-bearing peridotites and kimberlites revisited. *Contrib. Mineral. Petrol.* **142,** 603–625.

Griffin W. L., Rege S., Davies R. M., Jackson S., and O'Reilly S. Y. (2004) Trace element analysis of diamond by LAM ICPMS: Standardisation, results and direction. In *Proceedings of the 55th Diamond Conference,* pp. 6.1–6.5.

Gurney J. J. (1989) Diamonds. *Geol. Soc. Australia Spec. Bull.* **14,** 936–965.

Guthrie G. D., Veblen D. R., Navon O., and Rossman G. R. (1991) Sub-micrometer fluid inclusions in turbid-diamond coats. *Earth Planet. Sci. Lett.* **105,** 1–12.

Harris J. W. (1992) Diamond geology. In *The Properties of Natural and Synthetic Diamonds* (ed. J. E. Field), pp. 384–385. Academic Press,.

Harte B., Hunter R. H., and Kinny P. D. (1993) Melt geometry, movement and crystallization, in relation to mantle dykes, veins and metasomatism. *Phil. Trans. R. Soc. Lon. A Math. Physical Eng. Sci.* **342** (*1663*), 1–21.

Hauri E. H., Wang J., Pearson D. G., and Bulanova G. P. (2002) Microanalysis of delta C-13, delta N-15, and N abundances in diamonds by secondary ion mass spectrometry. *Chem. Geol.* **185,** 149–163.

Hayakawa S., Jia X. P., Wakatsuki M., Gohshi Y., and Hirokawa T. (2000) Analysis of trace Co in synthetic diamonds using synchrotron radiation excited X-ray fluorescence analysis. *J. Crystal Growth* **210,** 388–394.

Hervig R. L., Smith J. V., Steele I. M., Gurney J. J., Meyer H. O. A., and Harris J. W. (1980) Diamonds: Minor elements in silicate inclusions: Pressure dependent implications. *J. Geophys. Res.* **8,** 6919–6929.

Ionov D. A., Dupuy C., Oreilly S. Y., Kopylova M. G., and Genshaft Y. S. (1993) Carbonated peridotite xenoliths from spitsbergen—Implications for trace-element signature of mantle carbonate metasomatism. *Earth Planet. Sci. Lett.* **119,** 283–297.

Izraeli E. S., Harris J. W., and Navon O. (2001) Brine inclusions in diamonds: A new upper mantle fluid. *Earth Planet. Sci. Lett.* **187,** 323–332.

Izraeli E. S., Harris J. W., and Navon O. (2004) Fluid and mineral inclusions in cloudy diamonds from Koffiefontein, South Africa. *Geochim. Cosmochim. Acta* **68,** 2561–2575.

Johnson L. H., Burgess R., Turner G., and Harris J. W. (2000) Noble gas and halogen geochemistry of mantle fluids: Comparison of African and Canadian diamonds. *Geochim. Cosmochim. Acta* **64,** 717–732.

Jones A. P. (1989) Upper mantle enrichment by kimberlitic or carbonatitic magmatism. In *Carbonatites, Genesis and Evolution* (ed. K. Bell), pp. 448–463. Unwin Hyman.

Kirkley M. B., Smith H. S. and Gurney J. J. (1989) Kimberlite carbonates—A carbon and oxygen isotope study. In *Kimberlites and Relates Rocks* (ed. J. Ross), pp. 264–281. Blackwell.

Klein-BenDavid O., Izraeli E. S., and Navon O. (2002) Volatile-rich brine and melt in Canadian diamonds. *Geochim. Cosmochim. Acta* **66,** A403–A403.

Klein-BenDavid O., Izraeli E. S., Hauri E., and Navon O. (2004) Mantle fluid evolution—A tale of one diamond. *Lithos* **77,** 243–253.

Klemme S., Blundy J. D., and Wood B. J. (2002) Experimental constraints on major and trace element partitioning during partial melting of eclogite. *Geochim. Cosmochim. Acta* **66,** 3109–3123.

Lang A. R. and Walmsley J. C. (1983) Apatite inclusions in natural diamond coat. *Phys. Chem. Minerals* **9,** 6–8.

Latourrette T., Hervig R. L., and Holloway J. R. (1995) Trace-element partitioning between amphibole, phlogopite, and basanite melt. *Earth Planet. Sci. Lett.* **135,** 13–30.

Li C., Ripley E. M., and Mathez E. A. (2003) The effect of S on the partitioning of Ni between olivine and silicate melt in MORB. *Chem. Geol.* **201,** 295–306.

Litvin Y. A., Chudinovskikh L. T., and Zharikov V. A. (1998) Seed growth of diamond in the system $Na_2Mg(CO_3)_2$-$K_2Mg(CO_3)_2$-C at 8–10 GPa. *Doklady Akademii Nauk* **359,** 818–820.

McDonough W. F. and Sun S.-S. (1995) The composition of the Earth. *Chem. Geol.* **120** (228–253).

Mendelssohn M. J. and Milledge H. J. (1995) Geologically significant information from routine analysis of the mid-infrared spectra of diamonds. *Int. Geol. Rev.* **37,** 95–110.

Meyer H. O. A. (1987) Inclusions in diamond. In *Mantle Xenoliths* (ed. P. H. Nixon), pp. 501–522. Wiley-Interscience.

Moore K. R. and Wood B. J. (1998) The transition from carbonate to silicate melts in the CaO-MgO-SiO_2-CO_2 system. *J. Petrol.* **39,** 1943–1951.

Navon O. (1991) High internal-pressures in diamond fluid inclusions determined by infrared-absorption. *Nature* **353** (*6346*), 746–748.

Navon O., Hutcheon I. D., Rossman G. R., and Wasserburg G. J. (1988) Mantle-derived fluids in diamond micro-inclusions. *Nature* **335,** 784–789.

Pal'yanov Y. N., Sokol A. G., Borzdov Y. M., Khokhryakov A. F., and Sobolev N. V. (1999) Diamond formation from mantle carbonate fluids. *Nature* **400** (*6743*), 417–418.

Potts J., Thompson M., and Wilson S. (2002) GPROBE1—An international proficiency test for microprobe laboratories. *Geostand. Newslett.* **26,** 197–235.

Rege S., Davies R. M., Griffin W. L., Jackson S., and O'Reilly S. Y. (2003) Trace element analysis of diamond by LAM ICPMS: Preliminary results. In *Proceedings of the 8th International Kimberlite Conference,* p. FLA_0087. Mineralogical Society of America.

Resano M., Vanhaecke F., Hutsebaut D., De Corte K., and Moens L. (2003) Possibilities of laser ablation-inductively coupled plasma-mass spectrometry for diamond fingerprinting. *J. Anal. Atomic Spectrom.* **18,** 1238–1242.

Ryabchikov I. D., Edgar A. D., and Wyllie P. J. (1991) Partial melting in the system carbonate phosphate peridotite at 30 kbar. *Geokhimiya* **2,** 163–168.

Saxena S. K. (1989) The oxidation state of the mantle. *Geochim. Cosmochim. Acta* **53,** 89–95.

Schrauder M. and Navon O. (1994) Hydrous and carbonatitic mantle fluids in fibrous diamonds from Jwaneng, Botswana. *Geochim. Cosmochim. Acta* **58,** 761–771.

Schrauder M., Koeberl C., and Navon O. (1996) Trace element analyses of fluid-bearing diamonds from Jwaneng, Botswana. *Geochim. Cosmochim. Acta* **60,** 4711–4724.

Snyder G. A., Taylor L. A., Jerde E. A., Clayton R. N., Mayeda T. K., Deines P., Rossman G. R., and Sobolev N. V. (1995) Archean mantle heterogeneity and the origin of diamondiferous eclogites, Siberia—Evidence from stable isotopes and hydroxyl in garnet. *Am. Mineral.* **80,** 799–809.

Spetsius Z. V. (1995) Diamondiferous eclogites from Yakutia: Evidence for a late and multistage formation of diamonds (abstract). In *Proceedings of the 6th International Kimberlite Conference,* pp. 572–574.

Stachel T. and Harris J. W. (1997) Diamond precipitation and mantle metasomatism—Evidence from the trace element chemistry of silicate inclusions in diamonds from Akwatia, Ghana. *Contrib. Mineral. Petrol.* **129,** 143–154.

Stachel T., Harris J. W., Tappert R., and Brey G. P. (2003) Peridotitic diamonds from the Slave and the Kaapvaal cratons—Similarities and differences based on a preliminary data set. *Lithos* **71,** 489–503.

Stachel T., Viljoen K. S., McDade P., and Harris J. W. (2004) Diamondiferous lithospheric roots along the western margin of the Kalahari Craton—The peridotitic inclusion suite in diamonds from Orapa and Jwaneng. *Contrib. Mineral. Petrol.* **147,** 32–47.

Sweeney R. J., Prozesky V., and Przybylowicz W. (1995) Selected trace and minor element partitioning between peridotite minerals and carbonatite melts at 18–46 kb pressure. *Geochim. Cosmochim. Acta* **59,** 3671–3683.

Taylor L. A. and Anand M. (2004) Diamonds: Time capsules from the Siberian mantle. *Chem. Erde Geochem.* **64,** 1–74.

Taylor W. R., Tompkins L. A., and Haggerty S. E. (1994) Comparative geochemistry of West African kimberlites—Evidence for a micaceous kimberlite endmember of sublithospheric origin. *Geochim. Cosmochim. Acta* **58,** 4017–4037.

Thompson J. F. H. and Barnes S. J. (1984) The distribution of nickel and iron between olivine and magmatic sulphides in some natural assemblages. *Can. Mineral.* **22,** 55–66.

Walmsley J. C. and Lang A. R. (1992a) On sub-micrometer inclusions in diamond coat—Crystallography and composition of ankerites and related rhombohedral carbonates. *Min. Mag.* **56** (*385*), 533–543.

Walmsley J. C. and Lang A. R. (1992b) Oriented biotite inclusions in diamond coat. *Min. Mag.* **56** (*382*), 108–111.

Wang W., Moses T. M., and Shigley J. E. (2003) Physical and chemical features of a large coated natural diamond crystal. *Diamond Related Materials* **12,** 330–335.

Woolley A. R. and Kempe D. R. C. (1989) Carbonatites: Nomenclature, average chemical compositions and element distribution. In *Carbonatites—Genesis and Evolution* (ed. B. K.), pp. 105–148. Unwin Hyman.

Yaxley G. M. and Brey G. P. (2004) Phase relations of carbonate-bearing eclogite assemblages from 2.5 to 5.5 GPa: Implications for petrogenesis of carbonatites. *Contrib. Mineral. Petrol.* **146,** 606–619.

Zedgenizov D. A., Kagi H., Shatsky A. F., and Sobolev N. V. (2004) Carbonatitic melts in cuboid diamonds from Udachnaya kimberlite pipe (Yakutia): Evidence from vibrational spectroscopy. *Min. Mag.* **68,** 61–73.